4.5

AN ALGORITHM FOR OPERATIONAL WIND FIELD RETRIEVAL USING RADARSAT-1 SCANSAR IMAGES

Jochen Horstmann[1], Wolfgang Koch[1], Susanne Lehner[2], and Rasmus Tonboe[3]

[1]GKSS Research Center, Geesthacht, Germany
[2]German Aerospace Center, Oberpfaffenhoven, Germany
[3]Danish Meteorological Institute, Copenhagen, Denmark

ABSTRACT: An algorithm for retrieving mesoscale wind fields from ScanSAR data acquired aboard the Canadian satellite RADARSAT-1 is presented. The algorithm consists of two parts, one for wind direction and another for wind speed retrieval. Wind directions are extracted from wind-induced streaks, e.g., from boundary layer rolls, Langmuir cells or wind shadowing, which are approximately in line with the mean wind direction. Wind speeds are derived from the normalized radar cross section (NRCS) and image geometry of the calibrated ScanSAR image, together with the local wind direction using the semi empirical C-band model CMOD4. The CMOD4 was developed for the scatterometer operating at C-band with vertical polarization and has to be modified for horizontal polarization, which is performed by considering the polarization ratio according to Kirchhoff scattering. To verify the algorithm, wind fields were computed from several RADARSAT-1 ScanSAR images and compared to collocated results from the Danish high resolution limited area model. To estimate relative errors of wind speed due to uncertainties in wind direction and NRCS, sensitivity studies were performed.

1. INTRODUCTION

To date mesoscale wind fields are frequently computed by meteorological models or measured, e.g., by wind scatterometers (SCAT) with grid cells of the order of 10 km. However, to study processes in the boundary layer and model coastal processes, e.g., currents, waves, winds and related transport processes, finer spatial resolution is needed. Since the launch of the European remote sensing satellites ERS-1 and ERS-2, and the Canadian satellite RADARSAT-1, synthetic aperture radar (SAR) images have been acquired over the oceans on a continuous basis. Their independence on daylight and all-weather capability together with their high resolution and large spatial coverage make them to a valuable tool for measuring geophysical parameters like ocean surface winds, waves, and sea ice. The SAR aboard the Canadian satellite RADARSAT-1 operates in the C-band (5.3 GHz) at moderate incidence angles between 20° and 50°. For this electromagnetic wavelength and range of incidence angles the backscatter of the ocean surface is primarily caused by the small-scale surface roughness which is in resonance with the incidence radiation of the radar. The surface roughness is strongly influenced by the local wind field and therefore allows the backscatter to be a measure of wind.

In the past few years much effort has been undertaken to develop algorithms for derivation of wind vectors from SAR images. The wind direction can be retrieved from the direction of wind-induced streaks visible in most SAR images, which are approximately in line with the mean wind direction. The direction of these streaks can either be retrieved by using spectral methods [1, 2, 3], or by using a method based on derivation of local gradients [4]. The wind speed is derived from the measured normalized radar cross section (NRCS) using empirical C-band models for vertical polarized C-band SAR data [2, 3, 5], these models have been extended to horizontal (HH) polarization [6, 5, 7].

The first part of the paper introduces the investigated data sets and gives a brief description of the applied SAR wind retrieval method. Thereafter comparisons of RADARSAT-1 ScanSAR retrieved wind fields to results of the Danish high resolution limited area model (HIRLAM) are performed. Finally, the main sources of errors are discussed and estimated.

2. INVESTIGATED DATA SETS

The ScanSAR wide swath A images were acquired by the SAR aboard the Canadian satellite RADARSAT-1 which operates with the C-band (5.3 GHz) with HH polarization on a sunsynchronous orbit. The ScanSAR wide swath comprises four beams which cover four areas in range with sequential scans between incidence angles of 20° and 50°. Each processed image covers an area of approximately 500 × 500 km with a pixel size of 50 m. The resolution of the four beams differs from 86.5 to 146.8 m in range and 93.1 to 117.5 m in azimuth. All ScanSAR data were processed by Gatineau Processing Facility in Canada into calibrated ScanSAR images, with a nominal radiometric accuracy of ±1.35 dB.

HIRLAM is a mesoscale atmospheric model which is in operational use at the Danish Meteorological Institute (DMI). It is a semi-implicit model, with Eulerian advection and leapfrog time stepping [8]. For the Greenland area it was set up with a time step of 240 s and a horizontal resolution of 0.45°. The analysis of the model is performed every six hours using the optimum interpolation method, which is a statistical procedure to minimize the difference between observations and first guess from the model. The lateral boundary values for the model are obtained from the global model of the European Center for Medium Range Weather Forecast.

3. METHOD FOR WIND FIELD RETRIEVAL

The wind direction can be retrieved from the direction of wind-induced streaks visible in most SAR images, e.g., from boundary layer rolls, Langmuir cells, or wind shadowing, which are approximately in line with the mean wind direction. In a first method SAR sub-images are transformed into the wavenumber domain, where the wind direction corresponds to the direction perpendicular to the line connecting

the maxima of spectral energy. A spectral filter (at 500 to 1500 m wavelength) is applied to distinguish wind-induced streaks from ocean waves and from larger-scale atmospheric structures such as atmospheric gravity waves. Due to the symmetry of the spectrum, the wind direction can only be computed with a 180° ambiguity. The algorithm shows good results applied to ERS-1 and ERS-2 SAR images [3, 5]. The second method defines the wind direction as normal to the local gradients derived from smoothed amplitude images. Therefore the ScanSAR images are smoothed and reduced to an appropriate pixel size, e.g., 100 m, 200 m, and 400 m. From these pixels the local directions, defined by the normal to the local gradient is computed leaving a 180° ambiguity. From the resulting directions the most frequent and most probable local direction is selected concerning assumptions such as of the wind flux pattern. The method is described in detail by Koch [4].

The method for retrieving wind speeds from SAR is based on a model function relating the NRCS of the ocean surface to the local wind speed, wind direction versus antenna look direction and incidence angle. In general the model depends on radar frequency and polarization. For C-band with VV polarization the empirical model CMOD4 was especially developed for the SCAT aboard ERS-1 [9]. The CMOD4 has been applied successfully for wind speed retrieval from C-band VV polarized ERS-1 and ERS-2 SAR images [2, 3, 5]. For wind speed retrieval from C-band HH polarized SAR images no similar well developed model exists so that a hybrid model function is applied that consists of the CMOD4 and a C-band polarization ratio (PR), defined as VV/HH hereafter [6, 5, 7]. So far the PR is not well known and several different PR's are suggested which are mainly incidence angle dependent. In the study from Horstmann et al. [7] the PR was estimated RADARSAT-1 ScanSAR images collocated to ERS-2 SCAT their results showed that the PR is similar to that predicted by Kirchhoff scattering and a model suggested by Elfouhaily [10]. Similar results were obtained by Vachon and Dobson [11], who compared well calibrated RADARSAT-1 SAR images, at incidence angles between 20° and 48°, to buoy data. Therefore in this study the hybrid model function consisting of the CMOD4 and the PR according to Kirchhoff scattering is used,

$$PR = \frac{\left(1 + 2\,\tan^2\,\theta\right)^2}{\left(1 + \tan^2\,\theta\right)^2}, \qquad (1)$$

where θ is the incidence angle of radar beam.

4. EXAMPLE OF SCANSAR RETRIEVED WIND FIELD

In Fig. 1 a RADARSAT-1 ScanSAR image from the south tip of Greenland acquired on March 29, 2000 is shown. Along the east coast of Greenland a 20 to 50 km wide ice belt is visible, which is known to flow southward around Cape Farewell. In the entire image wind-induced streaks were detected at scales between 400 and 1600 m. The first method for measuring the orientation of the streaks, based on the direction of a spectral peak in the wave number domain, gave insufficient results. Applying the second method, based on local gradients, on a image smoothed to

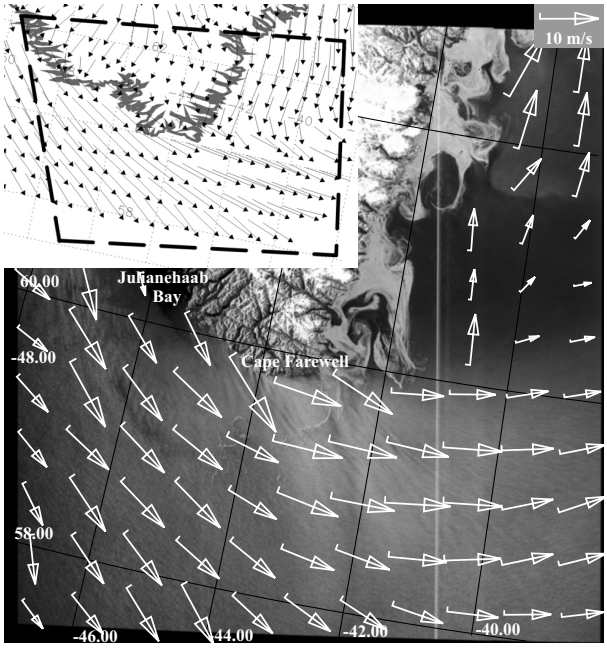

Fig. 1: Part of a RADARSAT-1 ScanSAR image from the south tip of Greenland. The Superimposed arrows represent the mean orientation of streaks in an area of 50 km × 50 km as computed from the local gradients. Local gradients were derived from the 200 m × 200 m smoothed RADARSAT-1 ScanSAR image. The wind field resulting from the atmospheric high resolution model, HIRLAM, are plotted in the upper left.

200 m × 200 m pixel-size gave the direction of the streaks visible at the corresponding scale (400 to 800 m). The resulting orientations of the streaks in an area of 50 km × 50 km are given by the superimposed arrows in Fig. 1, were the length of the arrows give the ScanSAR-retrieved wind speed. The directional ambiguity of wind direction was removed due to wind-shadowing visible in the lee of the coast in the Julianehaab Bay and considering a flow pattern over the entire image. It can be seen that retrieved wind directions represent the directions of the HIRLAM results. Unfortunately no wind-shadowing was visible east of Greenland to resolve the 180° ambiguity correctly. A detailed comparison of ScanSAR-retrieved wind directions to HIRLAM results will be carried out in near future.

5. COMPARISON OF SCANSAR-RETRIEVED WIND SPEEDS TO HIRLAM

To test the applicability of the hybrid model function for a large range of wind situations, a comparison was performed using a data set consisting of 9 RADARSAT-1 ScanSAR images. All images were acquired in the Cape Farewell area between January and August 1999, at approximately 20:30 UTC. For the comparison the 21:00 UTC wind forecast of the atmospheric model HIRLAM is used. The ScanSAR images were averaged to the grid of the HIRLAM model, resulting in an average grid cell size of approximately 28 km × 55 km. Wind speeds were retrieved from ScanSAR using the hybrid model function considering the PR accord-

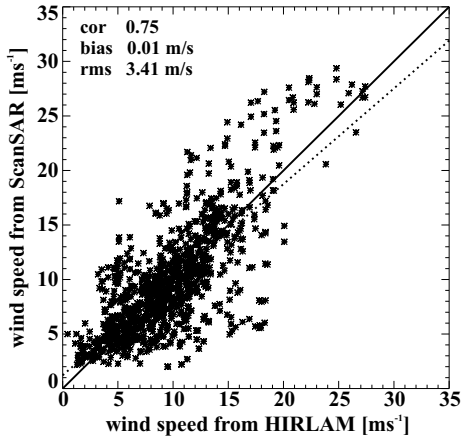

Fig. 2: Scatterplot of wind speeds from HIRLAM versus wind speeds from ScanSAR.

ing to Kirchhoff scattering. For each grid cell, the wind speeds were derived using the NRCS and incidence angle from the ScanSAR together with the wind direction from the HIRLAM model. Fig. 2 shows wind speeds retrieved from ScanSAR versus the collocated wind speeds resulting from HIRLAM. The comparison results in a correlation of 0.75 with a bias of 0.01 ms^{-1} and a root mean square error of 3.41 ms^{-1}.

To investigate the spatial distribution of main differences between the comparison of wind speeds from ScanSAR and HIRLAM, the differences were derived for each ScanSAR image at every grid cell. The main differences in wind speed occurred in the near range of the image (between 0 and 70 km), in the lee of the coast, and near to atmospheric structures, e.g., atmospheric fronts. The first is due to calibration inaccuracies, e.g., saturation of analogue to digital converter (ADC), which especially occur in the near range at high wind speeds. However, the other two phenomena cannot be described by calibration errors or a wrong choice of transfer function. In most images distinct differences in wind speed were observed near to the coast, especially in presence of wind shadowing, which shows that ScanSAR can significantly improve the information needed for modelling of wind fields, especially in such unattainable areas.

6. SOURCES OF ERROR

When computing wind speeds from ScanSAR images with the hybrid model function the accuracy is strongly dependent on the input to the algorithm (NRCS, wind direction and incidence angle). Main errors are caused by: the effect of speckle, uncertainty in wind direction and calibration accuracy of NRCS. The granular appearance of SAR images is the effect of speckle, a small-scale fluctuating component of the backscatter. In case of RADARSAT-1 ScanSAR images, speckle can be ± 3 dB on a single pixel which would thus cause a huge variation of wind speed. To reduce this effect the NRCS of the images have to be averaged over at least 1 km $\times$ 1 km.

The error in wind speed due to the accuracy of the NRCS is strongly dependent on the sensor performance and its calibration. In Fig. 3 the error in wind speed is plotted

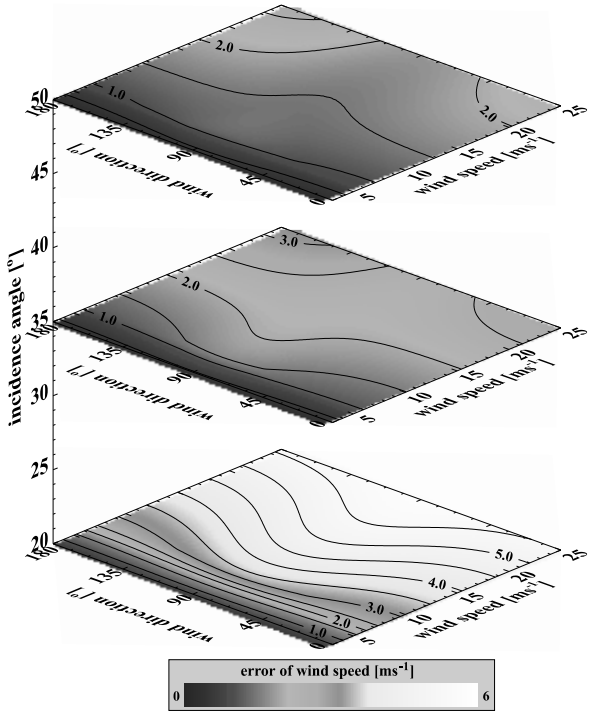

Fig. 3: Error in wind speed due to an uncertainty in NRCS of ± 0.5 dB.

assuming an accuracy of ± 0.5 dB. The computations were

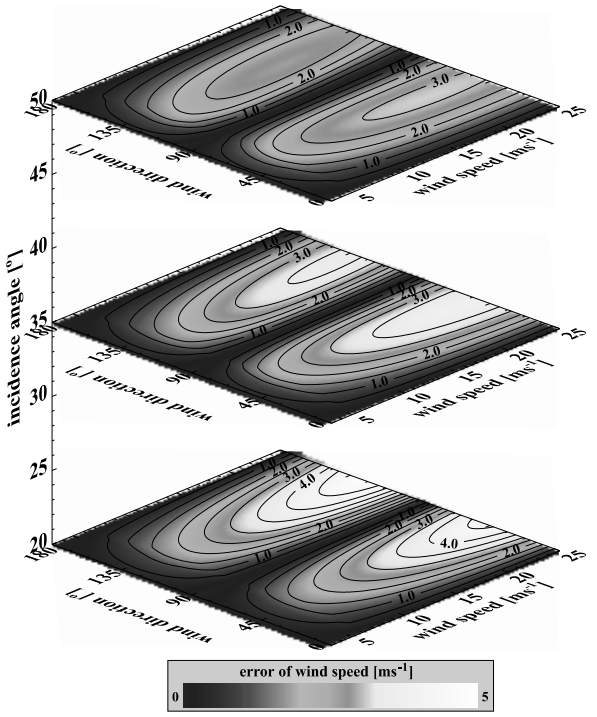

Fig. 4: Error in wind speed due to an uncertainty in wind direction of $\pm 10°$.

performed for incidence angles of 20°, 35°, and 50°, using the hybrid model function. The relative error decreases significantly with increasing wind speed and is slightly lower for cross wind then for up- and downwind. This behavior is similar for increasing incidence angles, though the error decreases significantly with increasing incidence angle.

Important for retrieval of the wind speed is the necessity to have information on wind direction. The NRCS is strongly dependent on wind direction and therefore uncertainties in wind direction can lead to significant errors in wind speed. The error in wind speed is plotted in Fig. 4 assuming an uncertainty in wind direction of $\pm 10°$. The computations were performed with the same model and the same ranges of input parameters used for the results of Fig. 3. The largest relative errors result from wind directions near to 45° and 135°, and near to 225° and 315°, due to the symmetry of the hybrid model function. With increasing incidence angle and for low wind speeds, the error increases. However, for higher wind speeds there is a distinct decrease of error with increasing incidence angle.

7. CONCLUSIONS

The application and usefulness of RADARSAT-1 ScanSAR images for mesoscale wind field retrieval over the ocean surface was shown. The operational use of ScanSAR-retrieved wind fields is planned at the Danish Meteorological Institute to help improve weather and especially ice drift forecast in the area around Greenland. ScanSAR-retrieved wind directions, using the local gradient method, are overall in good agreement with the wind directions resulting from the HIRLAM model. However, a thorough investigation of the ScanSAR-retrieved wind directions has to be performed. Comparison of ScanSAR-retrieved wind speeds to results of HIRLAM showed promising results. Investigation of the largest deviations in wind speeds between ScanSAR and HIRLAM showed a significant underestimation of the shadowing effect of Greenland by HIRLAM and calibration inaccuracies in ScanSAR data especially at near range (0 - 70 km), due to ADC saturation. The results of the sensitivity studies have shown that the best range of incidence angles for SAR wind speed retrieval are above 30°.

The advanced SAR (ASAR) aboard the European Environmental Satellite (ENVISAT), scheduled for launch in June 2001, will be capable to operate at wide swath mode as well, but with choice of polarization in addition. This will enable to investigate the polarization ratio in more detail and help improve wind retrieval from SAR. The algorithms and methods introduced here are an ideal preparation for the ENVISAT era to test the wind algorithms for the planned operational use of ENVISAT ASAR data at meteorological weather centers.

ACKNOWLEDGMENTS

The authors from the GKSS Research Center and from the German Aerospace Center (DLR) were supported by the German Bundesministerium für Bildung und Forschung (BMBF) in the framework of the project ENVOC.

REFERENCES

[1] T.G. Gerling, Structure of the surface wind field from Seasat SAR, J. Geophys. Res., vol. 91, pp. 2308–2320, 1986.

[2] P. W. Vachon and F.W. Dobson, Validation of wind vector retrieval from ERS-1 SAR images over the ocean, The Global Atm. and Ocean Syst., vol. 5, pp. 177–187, 1996.

[3] S. Lehner, J. Horstmann, W. Koch, and W. Rosenthal, Mesoscale wind measurements using recalibrated ERS SAR images, J. Geophys. Res., vol. 103, pp. 7847–7856, 1998.

[4] W. Koch, Semiautomatic assignment of high resolution wind directions in SAR images, in Proceedings of OCEANS 2000, Providence, Rhode Island, USA, 2000, vol. 3, pp. 1775–1782.

[5] J. Horstmann, S. Lehner, W. Koch, and R. Tonboe, Computation of wind vectors over the ocean using spaceborne synthetic aperture radar, John Hopkins APL Technical Digest, vol. 21, no. 1, pp. 100–107, 2000.

[6] D.R. Thompson and R.C. Beal, Mapping of mesoscale and submesocale wind fields using synthetic aperture radar, John Hopkins APL Technical Digest, vol. 21, no. 1, pp. 58–67, 2000.

[7] J. Horstmann, W. Koch, S. Lehner, and R. Tonboe, Wind retrieval over the ocean using synthetic aperture radar with C-band HH polarization, IEEE Trans. Geosci. Remote Sensing, vol. 38, no. 5, pp. 2122–2131, 2000.

[8] L. Wolters, G. Cats, N. Gustafsson, and T. Wilhelmsson, Data-parallel numerical methods in a weather forecast model, Applied Numerical Mathematics, vol. 19, pp. 159–171, 1995.

[9] A. Stoffelen, Scatterometry, Ph.D. thesis, Universiteit Utrecht, 1998, ISBN 90-393-1708-9.

[10] T. Elfouhaily, Physical modeling of electromagnetic backscatter from the ocean surface; Application to retrieval of wind fields and wind stress by remote sensing of the marine atmospheric boundary layer, Ph.D. thesis, Travail de recherche effectué au sein Département d'Océanographie Spatiale de l'Institut Français de Recherche pour l"Exploitation de la mer (IFREMER), Brest, France, 1997.

[11] P.W. Vachon and F.W. Dobson, Wind retrieval from RADARSAT SAR images: Selection of a suitable C-band HH polarization wind retrieval model, Canadian Journal of Remote Sensing, vol. 26, no. 4, pp. 306–313, 2000.